JACS
JOURNAL OF THE AMERICAN CHEMICAL SOCIETY

ARTICLE

pubs.acs.org/JACS

Mechanism of the Initial Stage of Silicate Oligomerization

Xue-Qing Zhang,[†] Thuat T. Trinh,[†,‡] Rutger A. van Santen,[†] and Antonius P. J. Jansen*[,†]

[†]Laboratory of Inorganic Chemistry and Catalysis, ST/SKA Eindhoven University of Technology, P.O. Box 513, 5600 MB Eindhoven, The Netherlands

[‡]Laboratoire de Chimie, Ecole Normale Supérieure de Lyon, 46, Allée d'Italie, 69364 Lyon Cedex 07, France

Supporting Information

ABSTRACT: The mechanism of the initial stage of silicate oligomerization from solution is still not well understood. Here we use an off-lattice kinetic Monte Carlo (kMC) approach called continuum kMC to model silicate oligomerization in water solution. The parameters required for kMC are obtained from density functional theory (DFT) calculations. The evolution of silicate oligomers and their role in the oligomerization process are investigated. Results reveal that near-neutral pH favors linear growth, while a higher pH facilitates ring closure. The silicate oligomerization rate is the fastest at pH 8. The temperature is found to increase the growth rate and alter the pathway of oligomerization. The proposed pH and temperature-dependent mechanism should lead to strategies for the synthesis of silicate-based materials.

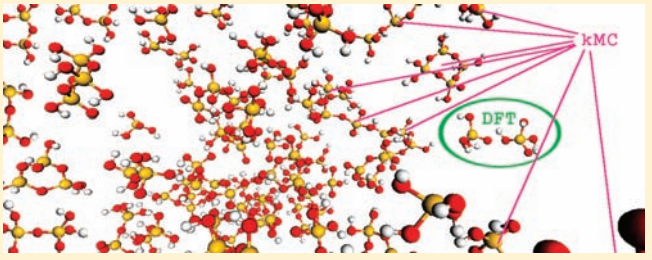

INTRODUCTION

Understanding how zeolites form is of fundamental scientific and technological importance.[1−3] Although numerous experimental and theoretical studies have been devoted to investigating the prenucleation process of siliceous zeolite formation,[4,5] the mechanisms governing the transformation of small silicate molecules into oligomers are still poorly understood.[2,6] The very early stages of solution oligomerization play a decisive role in determining the final structure.[7] Thus, higher levels of control over nucleation cannot be achieved without understanding the fundamentals of the elementary steps of silicate oligomerization. However, a detailed investigation of this process is still missing. The essential difficulty of studying the prenucleation process arises from the fact that the silicate oligomers are typically of the size of several $Si(OH)_4$ molecules, which is hardly accessible to most of the current experimental methods. Even if they are detected by microscopic techniques, the structural and reactive properties may not be distinguished due to their small size. Furthermore, some of the species exist for extremely short times and freely move throughout the available volume of solution, reducing the change of their appearance in the volume being examined.[7]

A variety of spectroscopic and scattering techniques have been used to study the silica-based condensation reactions,[8−10] but the information they give is generally incomplete and indirect.[11] Knight et al. used ^{29}Si nuclear magnetic resonance (NMR) spectroscopy to study condensed silicate species present in aqueous solutions.[10] Using mass spectrometry, Pelster et al. investigated the temporal evolution of silicate species during hydrolysis and condensation of silicates.[12] Depla et al. and Fan et al. presented UV−Raman investigations of the initial oligomerization reactions of the silica sol−gel process.[13,14] However, because of the multitude of simultaneous reactions in solution, it is difficult to extract information about individual events using only experimental data.[15]

Many models have been developed for modeling the early stages of solid formation. Wu and Deem introduced a Monte Carlo model for silicate solutions for investigation of the nucleation process during zeolite synthesis in the absence of a structure-directing agent.[16] A force field was used to simulate the formation of covalent bonds. Chemical potentials for Si and O are implicitly related to the pH of the system. The solvent effects were modeled by applying a distance-dependent dielectric constant. Schumacher et al. presented a Monte Carlo method for simulation of hydrothermal synthesis of periodic mesoporous silica (PMS).[17−19] Using simplified potentials this model enables the simulation, at an atomic level, of the entire process of the synthesis of templated PMS. The pH effects was taken into account implicitly in the reaction probabilities during the simulation. They also simulated the adsorption properties of the PMS models using Grand Canonical Monte Carlo simulation. More recently, Malani et al. presented a reactive Monte Carlo model, which is useful for modeling silicate oligomerization.[20] They have obtained agreement for the evolution of the Q_n distribution upon comparing the simulation results to experimental observations. Lattice-gas kinetic Monte Carlo models were also used to model the crystal nucleation. The method developed by Frenkel et al. has been used to give reliable results of the crystal nucleation and growth.[21−23] Jorge et al. presented a lattice-gas kinetic Monte

Received: November 18, 2010
Published: April 12, 2011

Carlo model describing the formation of silica nanoparticles.[24] They showed qualitative agreement with published experimental observations.

Here we compare our method with the models published earlier. Potentials or force fields have been used in all the modeling studies mentioned above to describe the particle interactions. The application of potentials allows for the simulation of large silicate clusters, which, however, falls short of detailed information of small oligomers. In this work DFT is used to predict the interaction and reaction details, which are the input of the subsequent kMC simulation. This allows us to track more detailed information, especially for the unstable species (such as the reactant complex and intermediate species). On the other hand, the calculation of a reaction barrier using DFT is easier than creating an efficient potential or force field for a certain type of material. This widens the range of applications of our model. The influence of water molecules is modeled explicitly in the DFT calculations and is incorporated in the rate constants in the kMC simulations. However, we stress that the particles are coarse-grained in the kMC simulations in order to make them computationally tractable. Thus, we cannot simulate the latter crystal-like zeolite frameworks. The off-lattice MC methods of Schumacher et al. and Wu and Deem mentioned above are equilibrium algorithms that are interpreted by rare event theory.[16−19] The drawback is that there is no real time in these methods. The same holds for the work of Malani et al.[20] An advantage of our kMC method is that the diffusion of molecules in the solution can be treated analytically. This allows the simulation itself to take little computer time or to be done on large systems. In the works of Frenkel et al. and Jorge et al., using a lattice gas, this is not the case and the simulations are much more time-consuming.[21−24] With the free energy barrier and a recrossing coefficient calculated by the Frenkel method, these results would give a rate. With a recrossing coefficient estimated from transition state theory, they would give an estimated rate. Another advantage of our model is that some important factors that influence the reactions in solution (pH and structure directing agents) can more easily be included (effects of structure directing agents will be shown in another work). Furthermore, the pH of the solution is modeled more explicitly than in the earlier works, as described in Model and Methods. Lattice-gas models also fall short of structural information of silicate oligomers, such as five-coordinated silicate, 3-ring, and 4-ring, which are important in the early stages of zeolite formation.

Many other theoretical methods, including electronic structure calculations[15,25,26] and molecular dynamics (MD),[27] have been used to probe the formation of zeolites and mesoporous materials. Typically it is difficult for MD methods to model chemical reactions. Information about the energetics of chemical reactions can be obtained by using DFT calculations, but kinetics cannot be predicted. Stable structures of silicate oligomers can be obtained from DFT calculations, but the most stable oligomers might not be the most preferable products. Moreover, DFT and MD methods are computationally very expensive and restricted to very small systems and short simulation times (on the order of pico- or nanoseconds); thus, relevant statistical information cannot be extracted. The time scale for the initial stages of zeolite formation is on the order of hours or even longer, which is not accessible to MD or DFT simulations.

Failure of the current techniques in investigating oligomerization from solution motivated us to develop a new approach. The effective modeling of silicate oligomerization in solution requires a method that can simulate events at microscopic length and macroscopic time scale. Given the experimental and theoretical difficulties, the off-lattice kinetic Monte Carlo method provides an alternative way to gain key insights into the prenucleation process. Here we use a kinetic Monte Carlo (kMC) theory,[28] which we call continuum kMC, to model silicate oligomerization reactions in water solution. In this theory, we take the general approach and apply it to reactions in solutions. We show that we can simplify the kMC simulations in such a way that the reactions can be determined independently from the simulations, just as for lattice-gas kMC. We treat the diffusion of molecules in the solution analytically. Because we then only need to simulate the reactions explicitly, the time that a simulation takes is drastically reduced. The model overcomes the limitations of the models mentioned above. In comparison to MD and DFT simulations continuum kMC can access longer time scales, are computationally inexpensive, and are more flexible than lattice Monte Carlo models. It is also more realistic than the methods of rate equations. In an early study,[28] we compared the results of rate equations and our method on a variation of the Lotka model. This model shows kinetics that is clearly different from that obtained from the rate equations. The reason for that is that the system is not homogeneous. For the case of silicate oligomerization reactions, the concentrations of some types of species are very low and fluctuate strongly, and thus the rate equations do not work as properly as off-lattice kMC. In this study, we compare the method with simulations of mean field approximations and show the differences.

The formation of zeolites consists of several stages: first, an oligomerization process which eventually leads to the formation of subcolloidal particles, second, the nucleation process, and finally crystal growth.[29] In this work we focus on the early stages of silicate oligomerization. Further development of a clearer picture of prenucleation may help determine the optimum conditions necessary for the effective organization within the silicate clusters.[7] In addition, a greater understanding of these processes may lead to an increase in the nucleation rate and avoiding the formation of undesired structures. The basic aim of this work is therefore to understand the mechanisms by which the silicate oligomers are formed in solution. The evolution of cluster-size distribution and the effects of pH and temperature on the oligomerization process are investigated.

This paper is organized as follows. Model and Methods describes the model we used for the silicate solution system and the simulation techniques employed. Results and Discussion presents the results obtained from the simulations. The results section begins with an analysis of the formation of silicate species implicated in the formation of zeolites. The effects of pH and temperature on the oligomerization process are discussed, and the preferred conditions for key silicate species are obtained. In Conclusions, we present our conclusions and a brief outlook about future goals.

MODEL AND METHODS

Theory of Continuum kMC. The kMC simulations were carried out using our newly developed continuum kMC.[28] We derived the method from first principles. We assume that diffusion leads to a Gaussian distribution for the position of the particles. This allows us to deal with the diffusion analytically, and we only need to simulate the reactive processes, so that the simulation itself takes little computer time or can be done on large systems. Of course, computational costs of kMC

are higher than those for macroscopic equations, but they are only modest compared to, for example, electronic structure calculations.

We have derived the method from the master equation that described the evolution of the system as hops from one minimum of the potential-energy surface to a neighboring one. This master equation is coarse-grained by using an analytical approach to the diffusion of the particles. This leads to a new master equation that describes only the chemical reactions, and no other processes. The diffusion is incorporated in the expression for the rate constants. The rate constants then depend on the distance between reacting particles at times before the reaction occurs. Solvent molecules need not be included explicitly in the simulations. Their effect can be incorporated in the rate constants as well. The reaction rate constants can be computed before a simulation is started and need not be computed on-the-fly as in other off-lattice kinetic Monte Carlo methods. The short-range interactions are included in the DFT calculations. Therefore, their effect is incorporated in the values of the rate constants for the reactions. Long-range interactions have been neglected. All oligomers are regarded as pointlike particles in our simulations. Thus, there is no excluded-volume effect that is present in lattice-gas kMC. We have compared our continuum kMC with lattice-gas kMC for the formation of dimers only and found that the effect of overlap between particles is negligible, provided the concentrations are not too high. The separation between the oligomers must be clearly larger than the size of the oligomers.

A basic flow of the simulation is as follows. An adaptation of the first-reaction method (FRM) is used due to the time dependence on the rate constants.[28,30] The method is adapted from the lattice-gas version.[28]

1. Initialize the simulation.
   1.1. Generate initial positions $r_{i,0}$ of the particles.
   1.2. Set the time t to some initial value t_0.
   1.3. Choose conditions when to stop the simulation.
   1.4. Make a list of particle positions (L_{part}) and times when the particles were at the corresponding positions.
   1.5. Make a list containing all reactions (L_{rx}) and times when the reaction will occur.
2. Determine the next reaction to occur. Determining the next reaction to occur involves looking in L_{rx} for the reaction that occurs first. We define t_n as the time of the nth reaction to occur. We have $t_i > t_j$ if and only if $i > j$.
3. Update the system, and repeat at 2, unless the end of the simulation is reached (e.g., final time reached or possible reactions exhausted). Updating the system when a reaction (e.g. number n) occurs involves the next series of steps.
   3.1. Determine the position where the reaction occurs.
   3.2. Remove the reacting particles from L_{part} and their reactions from L_{rx}.
   3.3. Add the particles that are formed to L_{part} and their reactions to L_{rx}.
   3.4. Change time to $t = t_n$.

More detailed information about the continuum kMC method can be found in ref 28.

An important advantage of continuum kMC is that solvent molecules can be removed from the simulations, which minimizes the number of particles that have to be simulated explicitly. If the solvent is only a spectator in the reactions, then we can practically ignore it. We need to know the relation between the kMC and the macroscopic rate constants. For a reaction A + B → C we have

$$\frac{d[A]}{dt} = -k[A][B] \tag{1}$$

with k being the macroscopic rate constant. In a kMC simulation we work with discrete particles. We have to multiply by L^3 with L being the side length of the simulation box. Then we have

$$\frac{dN_A}{dt} = -\frac{k}{L^3}N_A N_B = -\omega N_A N_B \tag{2}$$

where N_A and N_B are the numbers of A and B, respectively, and ω is the kMC rate constant. It is related to the macroscopic rate constant via $k = \omega L^3$ (note that the kMC rate constant can become dependent on the size of the simulation box).

For the case of silicate solution, water molecules participate in acid−base reactions. Silicate species can donate a proton to OH^- (or H_2O). For example, $Si(OH)_4$ is then transformed into $Si(OH)_3O^-$. There is also a reverse reaction where $Si(OH)_3O^-$ gets back a proton from H_2O (or H_3O^+). These processes can be given by the two example equations

$$Si(OH)_4 + OH^- \rightleftharpoons Si(OH)_3O^- + H_2O \tag{3}$$

with macroscopic rate constants k_1 and k_{-1} (reverse process) and

$$Si(OH)_4 + H_2O \rightleftharpoons Si(OH)_3O^- + H_3O^+ \tag{4}$$

with macroscopic rate constants k_2 and k_{-2} (reverse process). We can write macroscopic rate equations for these equilibria. Let us take the first case as an example:

$$\frac{d[Si(OH)_4]}{dt} = -k_1[Si(OH)_4][OH^-] + k_{-1}[Si(OH)_3O^-][H_2O] \tag{5}$$

The solvent actually takes part in the reaction, but if we do not want to include it explicitly in our simulations, then the rate constants above need to be modified. The expression above shows that we can accomplish this by replacing the equilibria above with

$$Si(OH)_4 \rightleftharpoons Si(OH)_3O^- \text{ (high pH)} \tag{6}$$

with rate constants $k_1[OH^-] = \omega_1 N_{(OH)^-}$ and $k_{-1}[H_2O] = \omega_{-1}N_{H_2O}$, $k_n = \omega_n L^3$ (see eq 2), and ω_n the kMC rate constants. N_{OH^-} and N_{H_2O} are the numbers of OH^- and H_2O in the simulation box, which we assume to be constant. We also have

$$Si(OH)_4 \rightleftharpoons Si(OH)_3O^- \text{ (low pH)} \tag{7}$$

with rate constants $k_2[H_2O] = \omega_2 N_{H_2O}$ and $k_{-2}[H^+] = \omega_{-2}N_{H^+}$. $[OH^-]$ and $[H^+]$ are determined by the pH of the solution, such as $[OH^-] = 10^{-7}$ mol/L at pH 7.

Model of the Oligomerization. kMC is very efficient, allowing for the simulations of large systems and long simulation times with modest computational work. In our simulations, the silicate-solution system contains up to 6000 silicate monomers, which is large enough to give good statistics, and the total simulation time is up to thousands of seconds, which is long enough for a realistic description of the initial stage of zeolite formation. The simulation box is 215 × 215 × 215 Å^3, and the initial monomer concentration is 1 mol/L, which is usually used in experiments. The reaction rate constants of all possible condensation and reverse reactions were obtained from DFT calculations, which were published earlier.[25,26] Two models were used to calculate the reaction barriers, one in which the solvent effect was treated by using the continuum solvation COSMO method implemented in the GAUSSIAN03 package,[25,31] which we call the COSMO model, and the other one in which Car−Parrinello molecular dynamics simulations were applied with explicit modeling of water molecules,[26,32] which we call the explicit-water model. Some of the activation energies in the explicit-water model were corrected,[26] because the silicate condensation reactions are endothermic in the Car−Parrinello molecular dynamics simulations (see the Supporting Information).

In an early study we reported, in agreement with other previously published works,[33] the reaction mechanism of oligomers containing up to four Si atoms, including the calculation of reaction activation energies.[25] To avoid unnecessary complexity, we have not considered the doubly ionized species, such as $[Si(OH)_2O_2]^{2-}$ and $[Si_2(OH)_4O_3]^{2-}$.

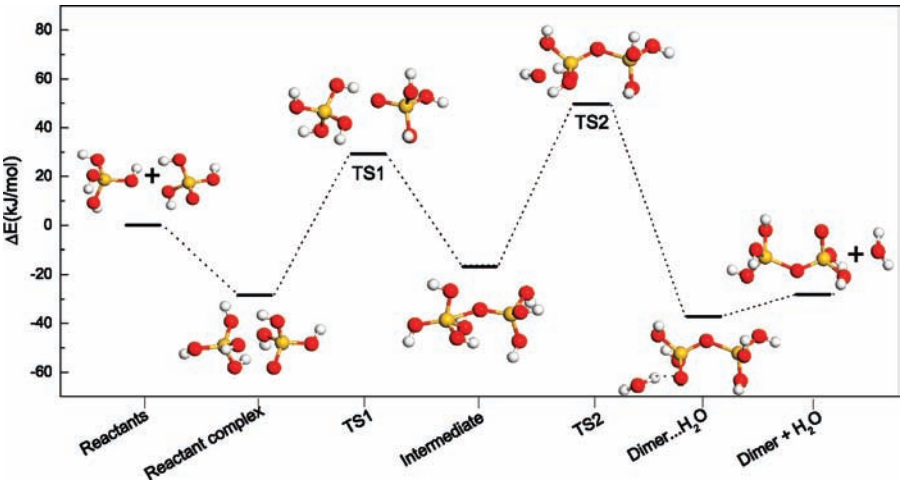

Figure 1. Schematic of the anionic mechanism of the dimerization reaction.

Even though doubly ionized species exist at very high pH, they are relatively unreactive in oligomerization.[34]

It has been shown that there are two different mechanisms: one in which the growing oligomer is negatively charged, as shown in Figure 1, and a neutral one in which all oligomers are neutral, as shown in Figure 2.[25] In a high-pH environment, the system is dominated by anionic species. Thermodynamic calculations show that in solution the OH^- ion will deprotonate the monomeric species to form the mono-charged anion $[Si(OH)_3O]^-$. The condensation reactions proceeded through a two-step mechanism with formation of a pentacoordinated intermediate, as shown in Figure 1. The first step is the formation of the SiO−Si bond between two monomers, and the second step is the removal of water to form the dimer species. In the first step, the anion $[Si(OH)_3O]^-$ will approach the monomer at a minimum distance to form a structure stabilized by three strong hydrogen bonds, which we call reactant complex, as described by the equations in the Supporting Information. The transition state corresponds to formation of the SiO−Si bond.[25] In this step, a reaction intermediate, which we call intermediate species, is formed with a pentacoordinated silicon. This was also reported by other researchers.[33] Hydrogen is transferred at the same time that a hydroxyl group starts to leave. As a result, the water molecule will be the leaving group and the product is again an anion that can either form a neutral dimer or initiate another condensation reaction to form a trimer.

The dimerization reaction can also occur via neutral reactant species, as shown in Figure 2. Two molecules approach through formation of hydrogen bonds at a minimum distance. This complex rearranges via a transition state with an intermolecular hydrogen transfer. The activation energy of this step is very high, due to strong interference of the hydroxyl proton. After hydrogen transfer, the water fragment leaves the molecule to form the dimer. The 5-fold silicon complex is not observed in this neutral route with lateral attack. The reaction for two anionic monomers (both reactants are charged), which we call a double-anionic mechanism, is rather unfavorable.[5,25] The pathway of trimerization and tetramerization is the same as that of dimerization.

Formation of the three-membered ring (3-ring) has been suggested before to occur via an intramolecular condensation reaction. Intramolecular hydrogen bridges between the hydroxyl groups of the molecules have to be broken to create a geometry so that internal ring closure can actually happen. This causes the unfavorable energies of intermediates (a pre-transition-state configuration) and the intermediate with five-coordinated Si.[25] The ring closure reaction may also take place via a hydrogen transfer mechanism between neutral species. The neutral

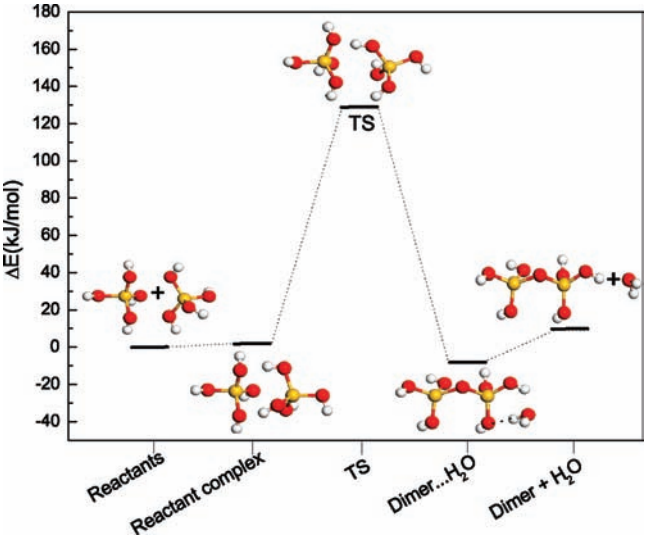

Figure 2. Schematic of the neutral mechanism of the dimerization reaction.

linear trimer changes conformation. The two ends of the chain approach each other. For the transition state, which is very similar to the case of the dimer, a hydrogen transfers to a hydroxyl group. After that, a water molecule will leave the cluster and a 3-ring is formed. The case of four-membered-ring (4-ring) formation is similar to that of the 3-ring mechanism.

The formation of silicate oligomers, with activation energies and reaction rate constants, is described in the Supporting Information.

RESULTS AND DISCUSSION

COSMO and Explicit-Water Model at Neutral pH. In our kMC simulation, the initial concentration of silicate monomers is 1 mol/L. The formation of zeolite particles is initiated when the solution is heated to a temperature of 350 K.[29] The temperature in this simulation is therefore set at 350 K. The rate constants are shown in Table 1 in the Supporting Information. Figure 3 shows the concentration of branched tetramers as a function of time. It is clear that the system almost fully transformed into branched tetramers (about 87% after 100 s) for the COSMO model, while

dx.doi.org/10.1021/ja110357k |J. Am. Chem. Soc. 2011, 133, 6613–6625

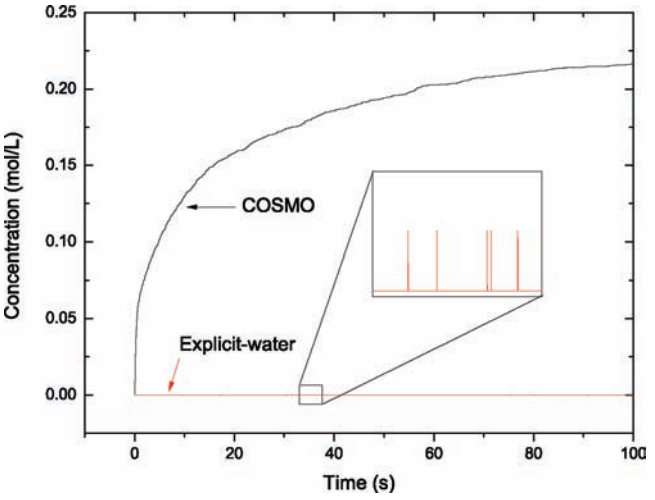

Figure 3. Concentration of branched tetramers as a function of time at pH 7 and temperature 350 K. The rate constants were obtained from the COSMO model. The height of the peaks in the insert is 1.6×10^{-4} mol/L and corresponds to the formation of one molecule.

the explicit-water model shows the near absence of branched tetramer. Experimentally, there are many other species, such as 3-ring and 4-ring species. This reveals that the COSMO model is inadequate in modeling silicate oligomerization in water, which was also predicted by other researchers.[11] A number of calculations of silicate oligomerization from water solutions were recently done by using the COSMO model.[15,25,35] How the environment, especially the solvent, can be adequately represented remains somewhat problematic. In the modeling of anionic silicate species by Catlow et al. it did not prove possible to provide a sufficiently detailed representation of the solvent to obtain results that were comparable with experiment.[11] To model the solvent more accurately, Catlow et al. then treated a few water molecules explicitly, which create the first solvation layer around the anion. The remainder of the solvent was modeled by the COSMO approach. Excellent results for the deprotonation of the silicate monomer were then obtained.[11] To study the influence of solvation on silicate oligomerization reactions, Schaffer et al. used a hybrid implicit/explicit hydration model that explicitly accounted for water in the calculations. Their results on the silicate dimer cluster revealed a marked change in both the mechanism and energetics of the reactions.[33] More recently, we reported the role of water in silicate oligomerization reactions, in which all the water molecules were modeled explicitly.[26] The results for the kinetics based on that approach are discussed in the next section. The inclusion of explicit water molecules changes the kinetics of the reactions. Formation of some of the species becomes relatively unfavorable. The most distinct case is the branched tetramer. There is a near absence of branched tetramer when the water molecules are treated explicitly, due to the fact that the formation of branched tetramers is rather unfavorable in this case. Consequently, formation of other species, 3-ring and 4-ring, becomes more favorable, as shown below.

Explicit-Water and Mean-Field Model at Neutral pH. The following kMC simulations were done on the basis of the parameters shown in Table 2 in the Supporting Information, which were obtained from the explicit-water model. The kMC simulation starts with 6000 silicate monomers, and the simulation box is $215 \times 215 \times 215$ Å^3. The pH of the solution determines the number of OH^- and H_3O^+ ions and consequently determines the conversion rate of neutral and anionic species. pH 7 and temperature $T = 350$ K are used for the first simulation, and we will take this simulation as reference for simulations with different pH and temperature.

Figure 4 shows the concentration of monomeric (neutral and anionic) and linear species (including dimer, trimer, and tetramer) as a function of time, in comparison with results from mean field approximation. Monomeric species are initially abundant; thus, dimerization is the dominant process. From the curve we can see the fast consumption of monomeric species. The system almost runs out of free monomeric species after 0.005 s, containing instead many small silicate oligomers as described below. Although monomeric species are produced by hydrolysis reactions, only a few of them can be observed, because the hydrolysis process is slow, while the produced monomeric species are consumed immediately by oligomerization reactions. This suggests that the monomeric species are more reactive than highly condensed oligomers.

The dimer is the first stable product of oligomerization. The process from monomer to dimer through two transition states is very fast. It is finished in 0.005 s. From 0.005 to 0.05 s, the dimer dominates the species population. After dimerization three-membered silicon species (linear trimer and 3-ring) emerge. However, the concentrations are low and the species do not exist long. The linear trimer participates in two types of reactions. It can either further oligomerize to form the linear tetramer (or branched tetramer) or form a 3-ring by ring closure. The linear trimers are therefore consumed quickly. The linear tetramer is the largest linear species in this model; the only route available for consumption of linear tetramers is ring closure. Thus, it can only form 4-rings rather than convert into a linear pentamer (larger species will be considered in our future work). After 0.1 s, the linear tetramer becomes dominant. Linear trimers can easily be converted, and the linear growth is favored. This suggests a clear tendency to form linear tetramers. The change in concentration becomes small after about 0.5 s. This is the first period of interest, which we call phase A.

We also did simulations with the mean field approximation for comparison to continuum kMC. The rate constants used in the mean field simulations are the same with those of kMC, except for the volume dependence of kMC rate constants for bimolecular reactions (see Model and Methods). Figure 4 shows clear differences between the two models. The most distinct difference is that the consumption of monomers (see Figure 4a) and formation of linear tetramers (see Figure 4c) are faster for the mean field approximation. The reason for this is that the species are assumed to distribute homogenously and the diffusion is assumed to be infinitely fast in the mean field simulations, while in the continuum kMC simulations the particles have to diffuse to get close enough before they are able to react. Thus, the linear growth, the bimolecular reactions, are slower for continuum kMC than for mean field.

Ring structured species are very important to zeolite formation. The 3-ring is the smallest closed structure that can be formed in a silicate structure. The 4-ring is commonly found in most of the zeolitic structures; 61 zeolites have the 4-ring as part of their structure.[36] From Figure 5 we can see that the concentration of the 3-ring follows that of the linear trimer with only a small delay. This suggests that the 3-ring formation is easy; meanwhile, it is also easy for a 3-ring to reopen again to form a

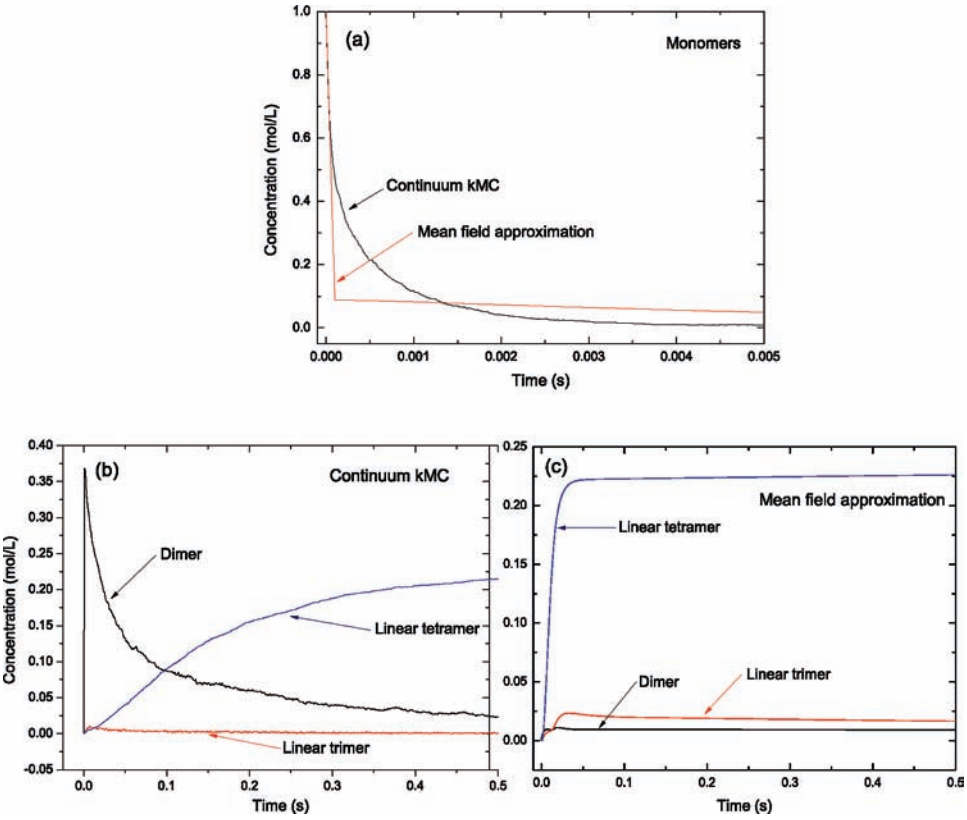

Figure 4. Concentration of monomers (a) and linear species (b) as a function of time at pH 7 and temperature 350 K (explicit-water model) in comparison with results from mean field approximation (a and c).

linear trimer. On the other hand, further linear growth leading to the linear tetramer is more favorable. Therefore, only a few three-membered silicon species are left after 0.5 s. This is consistent with published experimental results. NMR studies of reaction gels find solution-phase 3-rings.[37] However, the presence of such rings in zeolitic structures is rare. Our calculated results reveal that 3-rings are easy to reopen to support formation of 4-rings. The 3-rings do not directly participate in the growth of zeolite frameworks but serve as a source for the growth of larger species. Maybe this is why there are very few 3-rings present in the zeolite frameworks. Small species are consumed rapidly. This is again consistent with published experimental studies. Icopini and co-workers[38] reported that $[SiO_2]_{n\leq 3}$, where the subscripted n equals the number of silica tetrahedra in the polymeric molecule, decreases rapidly and approaches constant values soon after the beginning of the experiment.

4-rings emerge at the same time as linear tetramers (see Figure 5). The concentration of linear tetramers keeps increasing in the first 0.5 s, indicating that linear growth is faster than 4-ring formation. Unlike the situation of 3-rings, the concentration of 4-rings does not follow that of the linear tetramer. This indicates that both the formation and ring reopening for a 4-ring are more difficult than for a 3-ring, and the 4-ring is more stable than the 3-ring. The stable structure makes the 4-ring a popular structure in the zeolite frameworks.

The average particle size increases rapidly during the first 0.5 s. After that, the oligomerization process is dominated by 4-ring formation. This is in agreement with UV−Raman studies. Depla et al. have found that the 4-rings are the dominant species in the initial oligomerization of the silica sol−gel process.[13] The 4-rings are formed rapidly at early times, during which the system has abundant supporting species. After 300 s about 95% of the silicate species are transformed into 4-rings, and the system achieves equilibrium. This is the second period of interest, which we call phase B. At the end of the simulation the rates of the forward and reverse reactions are equal and the system is at a steady state. It is also possible to form larger species such as a pentamer, hexamer, etc. In that case some amount of 4-rings might be consumed, but in this model four-membered oligomers are the largest molecules considered.

The presence and formation mechanism of branched tetrameric species in the early stage of silicate oligomerization is still problematic. Pereira et al. showed that it is much easier to form linear than branched tetramers.[39] We have also found that the formation of linear tetramers and 4-rings is favored over that of branched tetramers.[26] This demonstrates that the formation of branched tetramer is rather unfavorable. The formation of branched tetramer[25,26,39−41] and branched cyclic tetramer (a 3-ring condensed with a monomer)[12,33,37,39,42−44] has been reported by a number of studies. Using density functional theory, Pereira et al. reported structural and energetic properties of both branched and branched cyclic tetramers.[39] They found that the branched tetramer is more stable than the branched cyclic tetramer. Schaffer et al. reported in more detail the formation of branched cyclic tetramers by three pathways.[33] They found that the pathway from a branched tetramer is the most favorable. In this work we found that the formation of branched tetramers is very unfavorable. Therefore, the formation pathway of branched cyclic tetramers from branched tetramers is not operable (because the concentration of reactants is very low), although the activation energy of this pathway is low.

dx.doi.org/10.1021/ja110357k |J. Am. Chem. Soc. 2011, 133, 6613–6625

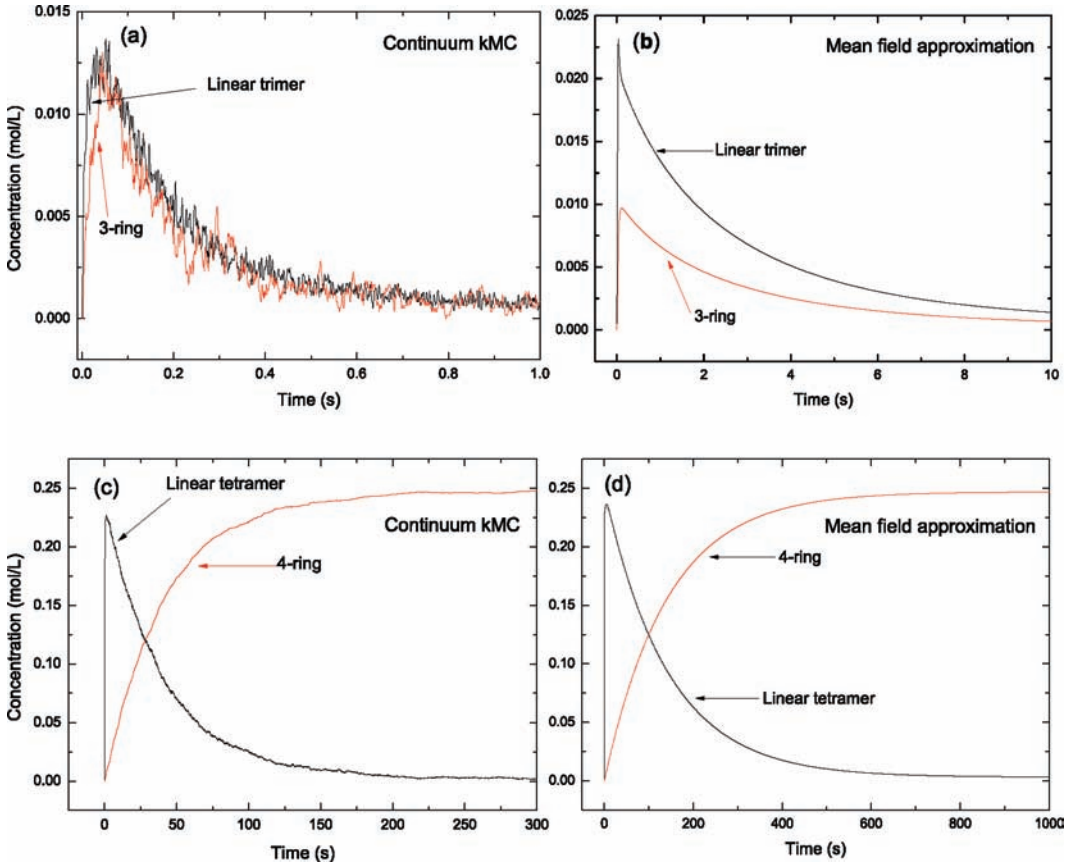

Figure 5. Formation of 3-rings (a) and 4-rings (c) at pH 7 and temperature 350 K (explicit-water model) in comparison to the results from a mean field approximation (b and d).

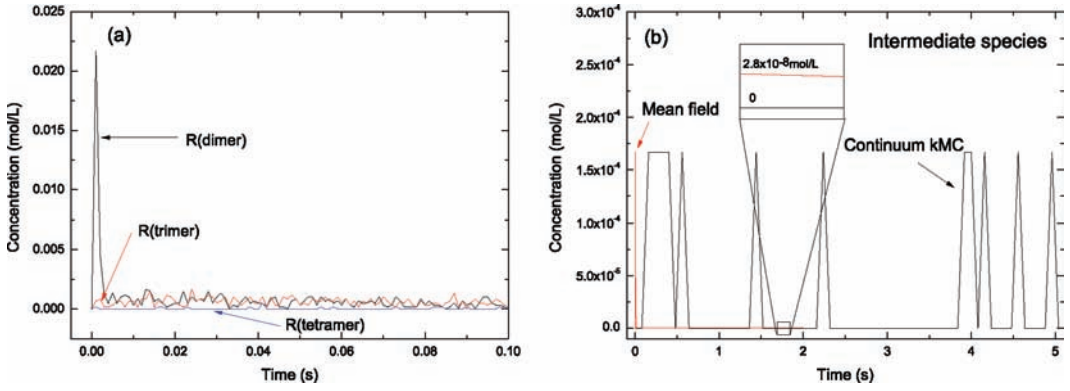

Figure 6. Concentration of reactant complexes (a) and intermediate species (b) as a function of time at pH 7 and temperature 350 K (explicit-water model).

Figure 5 shows a clear difference with the mean field approximation. Apart from the fluctuations, the values of concentration and the time scales are also different. The concentration of linear trimers is about two times that of 3-rings. The transformation from linear trimer/tetramer to 3-ring/4-ring is slower than that of continuum kMC. The reason is explained below.

Figure 6 shows the concentration of the unstable species. The reactant complex of the dimer, trimer, and tetramer are symbolized by R(dimer), R(trimer), and R(tetramer), respectively. Apparently, reactant complexes are not stable. More R(dimer) is formed in the first 0.002 s, due to the fact that the supporting species (monomers) is more abundant. The sharp increase in concentration of R(dimer) corresponds to the fast decrease of monomers. Figure 6 shows only the intermediate that leads to the dimer. The concentration changes of the other intermediate species (not shown here) are similar to the curve shown in Figure 6. It is apparent that the intermediate species are even less stable than the reactant complexes. The concentration shows only fluctuations. They exist for extremely short times, and they will not be detectable experimentally. The peak values of the concentration of the two models are almost the same: 1.6×10^{-4} mol/L, as shown in Figure 6. These are in good agreement. However, for the results of mean field simulation, the concentration keeps constant value (very low) after the first peak.

dx.doi.org/10.1021/ja110357k |*J. Am. Chem. Soc.* 2011, 133, 6613–6625

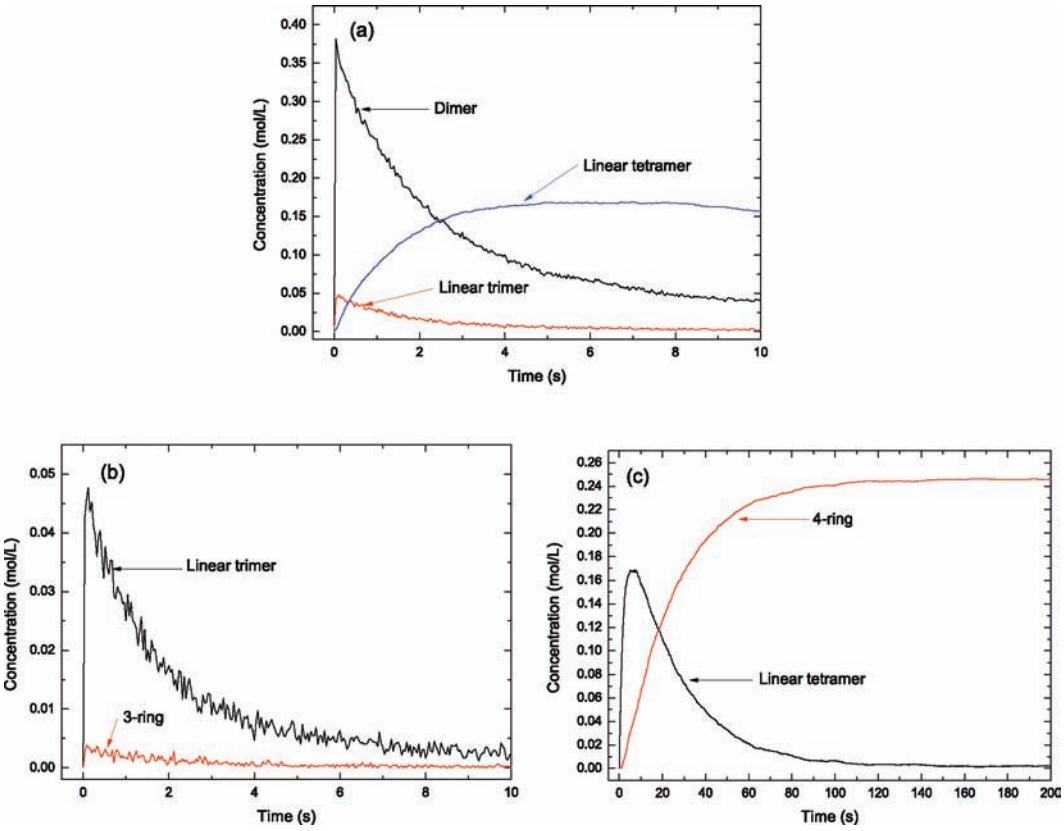

Figure 7. Evolution in the concentration of key species: linear species (a), formation of 3-ring (b), and formation of 4-ring (c), at pH 8 and temperature 350 K.

This is the reason the ring closure is slow for the mean field simulations. The ring closure reactions that occur through a intermediate are always unimolecular reactions. The particle simply diffuses and then reacts at whatever place it will be; it does not depend on the rate of diffusion. Therefore, the 3-ring and 4-ring formations from kMC are faster than those from mean field simulations. The particles are modeled explicitly in the kMC simulations. For the case of unstable species, such as intermediate species, the concentration is either zero or nonzero in the kMC simulations. However, in the mean field approach, the concentration is always nonzero (very low concentration). Mean field assumes a homogeneous distribution of reactants and an absence of fluctuations. However, this is not the real case. In this work we show that the heterogeneous distribution and the fluctuations are important. The continuum kinetic Monte Carlo simulations are a more realistic representation of the experimental situation.

Explicit-Water Model at Different pH and Temperature Conditions. *High pH.* For the case of high pH, the evolution of monomers, reactant complexes, and intermediate species are similar to those at neutral pH and are thus not shown in the following subsections.

Figure 7 shows how the concentration of key silicate species changes with time at pH 8. The formation of dimers is similar to the case of neutral pH. The consumption needs a longer time than at pH 7, as indicated by the curves. The dimers are mainly consumed by further linear growth, while the linear growth is slower at pH 8 than at pH 7. Linear tetramers need 2.5 s to become dominating, which is longer than at pH 7. Phase A lasts longer. This is due to the fact that more species are ionized at pH 8, which consequently results in the insufficient supply of neutral monomers, and thus the linear growth (a neutral species reacts with an anionic species) becomes slower. The formation of 3-rings is different from that at neutral pH. High concentrations of linear trimer do not lead to pronounced formation of 3-rings in the first 2 s, as can be seen from Figure 7. This demonstrates that the linear trimer prefers further linear growth and a consequent 4-ring formation rather than 3-ring formation at high pH, and thus the formation of 3-rings becomes unfavorable. There are fewer linear tetramers formed at pH 8. Interestingly, phase B is shorter at high pH, although the earlier phase A is longer. It is noteworthy that the process of transformation from monomers to 4-rings at high pH is different. At near neutral pH, the silicate species are first almost fully transformed into linear tetramers, followed by 4-ring formation. At high pH, these two processes, linear growth and 4-ring formation, occur simultaneously. The reason for this is that the linear growth is dominated by the anionic mechanism (neutral species react with anionic species). Neutral pH yields a favorable ratio of neutral/anionic species for linear growth. However, the ring closure occurs mainly through a single anionic linear species. At high pH, there are more anionic species, which consequently increases the rate of ring closure. Therefore, the formation of 4-rings is faster at high pH (pH 8), and this reduces the temporary concentration of linear tetramer.

We then increase the pH to 9 (results are shown in Figure 8). There are fewer linear species formed with respect to the results of pH 8. Linear growth is slow and unfavorable at pH 9. This is again because there are fewer neutral species at high pH. Phase A is much longer. A number of linear trimers are formed, which,

dx.doi.org/10.1021/ja110357k |*J. Am. Chem. Soc.* 2011, 133, 6613–6625

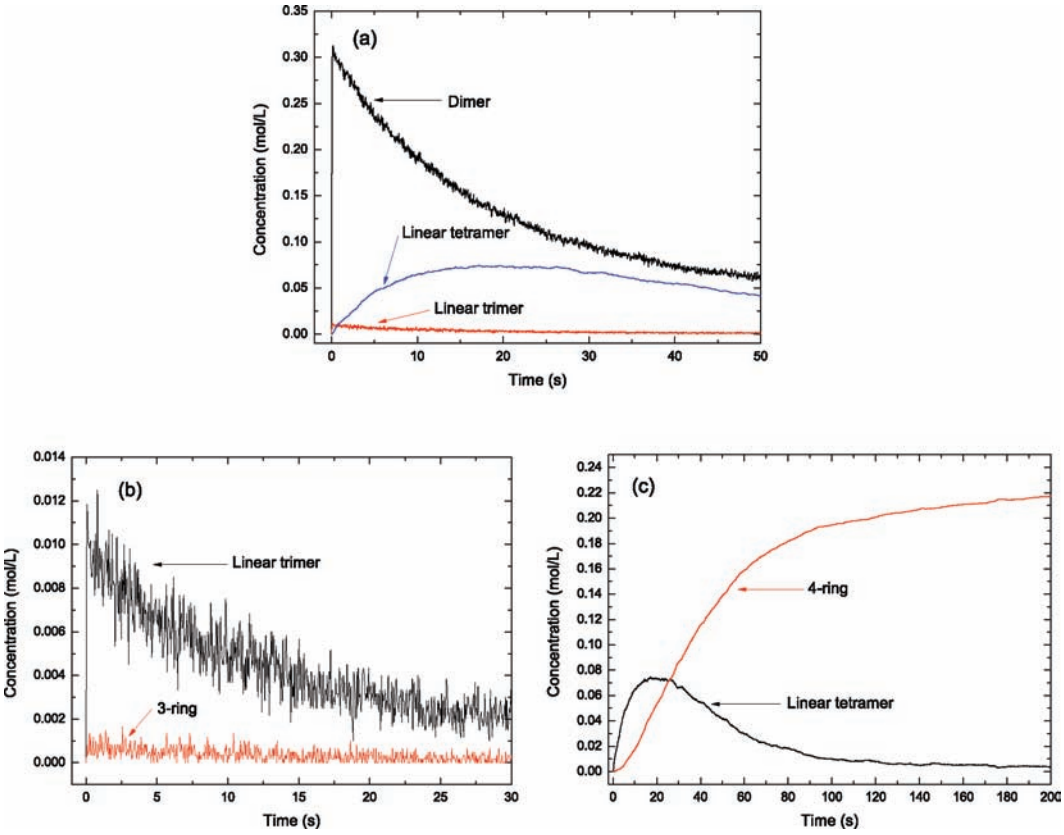

Figure 8. Evolution in concentration of key species: linear species (a), formation of 3-ring (b), and formation of 4-ring (c), at pH 9 and temperature 350 K (explicit-water model).

however, prefers further linear growth rather than ring closure. Thus, a low concentration of 3-rings is found. The ring closure prefers high pH; thus, the 4-ring formation should be faster at higher pH. However, phase B becomes longer at pH 9. This is due to linear growth being very slow (again due to insufficient supply of neutral monomers), and the 4-ring formation is limited by the formation of linear tetramers. The formation of both linear and ringed species is slower when the pH is increased to 10 (data not shown here); the population is dominated by the small species. Because of this, most of the species are anionic, and thus the linear growth is rather unfavorable at pH 10. The rate-determining step is the linear growth at high pH.

From the results presented above, we can conclude that the size of the silicate oligomers decreases with increasing pH (from 8 to 10). The same trend was found for larger silicate clusters in experimental studies. The cluster size was reported to decrease with pH.[24,45,46] Using in situ small-angle X-ray scattering (SAXS) and small-angle neutron scattering (SANS) Fedeyko et al. studied the formation of silicate nanoparticles in basic solutions of tetraalkylammonium cations (TAA).[45] They found that the particles have a core−shell structure with silica at the core and the TAA cations at the shell. The particle core size is nearly independent of the size of the TAA cation but decreases with pH, suggesting that electrostatic forces are a key element controlling their size and stability. Using a lattice model Jorge et al. studied the formation of silicate nanoparticles.[24] They found that more of the neutral silica monomers become ionized at high pH. A consequence of this is a significant increase in the particle charge on the surface and subsequent coverage by TPA cations. This layer is stabilized by electrostatic attractions between these cations and the negatively charged silica surface. Therefore, higher pH means that a protective TPA layer forms, hence inhibiting growth.[24] The silicate clusters of the published works above are larger and on the scale of several or tens of nanometers. However, no details of this have been reported before for small silicate oligomers. In this work, we found the same trend, but for a different reason. At high pH, the growing oligomers are anionic, the small species are also anionic, and thus the oligomerization can only occur through the double-anionic mechanism. The activation barrier for this is very high.[5,25] The high activation barrier of the double-anionic mechanism prevents the oligomers from further growing at very high pH. Therefore, the decrease in cluster size with pH is due to the high activation barrier of the double-anionic mechanism. This may also play a role in the growing mechanism of larger clusters and may account for the phenomenon that cluster size decreases with increasing pH to some extent.

Comparing the transformations from linear tetramer to 4-ring at different pHs, we can see a shift in the peak of linear tetramer to lower concentration as the pH increases. This means that the formation of linear tetramer is more favorable at low pH. Different from the situation of neutral pH, the increase in concentration of 4-rings is accompanied by a decrease in concentration of linear species, including dimer, linear trimer, and tetramer. The distribution of species is wider. This means that the formation of 4-rings is limited by the linear growth. This trend increases with increasing pH.

The changes in concentration collected at high pH showed significant differences with respect to those collected at neutral

dx.doi.org/10.1021/ja110357k |*J. Am. Chem. Soc.* 2011, 133, 6613–6625

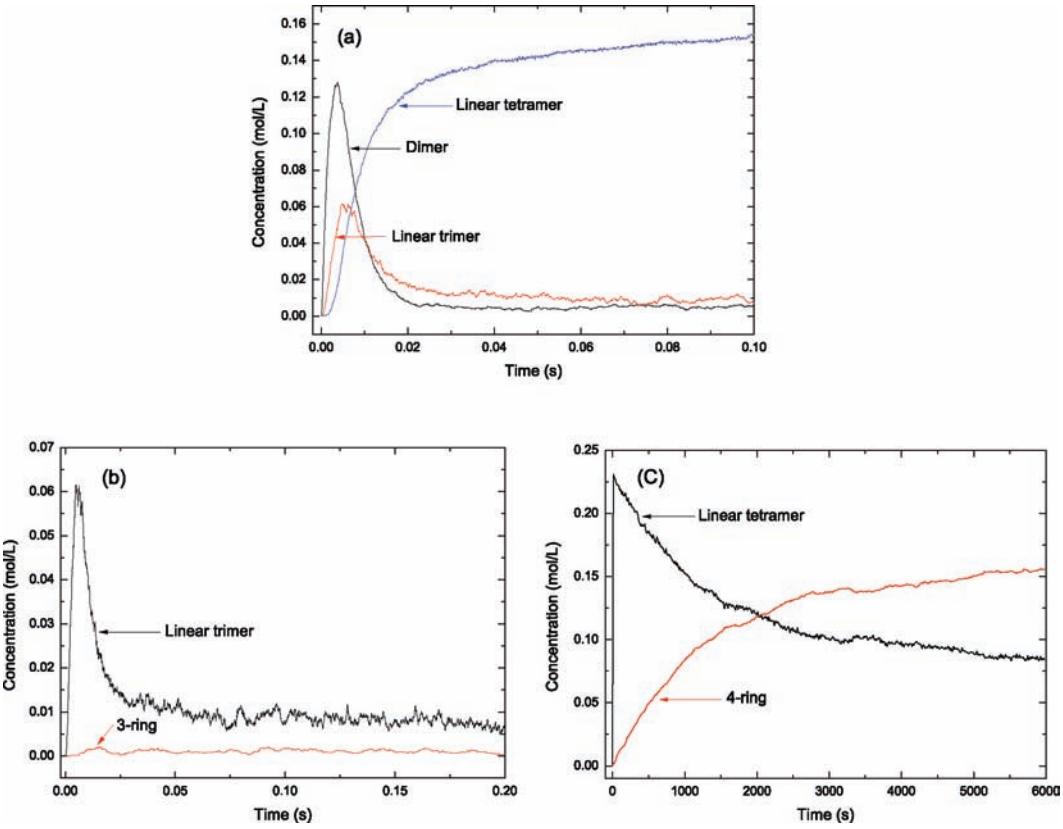

Figure 9. Evolution in concentration of key species: linear species (a), formation of 3-ring (b), and formation of 4-ring (c), at pH 6 and temperature 350 K (explicit-water model).

pH. The maximum values of concentration for the 3-rings are considerately higher at neutral pH. This means that the high pH does not favor formation of 3-rings but does favor 4-ring formation. An interesting finding at pH 8 is that the formation of 4-rings is most rapid, indicating a faster particle growth at pH 8 than at pH 7 and 9. At pH 7, the ring closure is slow, and at pH 9, the linear growth is slow, while at a pH value of 8, the molar ratio between neutral and anionic species makes the anionic mechanism of linear growth and ring closure the most favorable choice. This is consistent with results reported by Tleugabulova et al.[47] Using fluorescence anisotropy decay analysis Tleugabulova and co-workers evaluated formation and growth mechanisms of silicate. They found a faster particle growth at pH 8.2 than at pH 9.2 and more rapid condensation of silicate as the pH approaches neutrality. Icopini et al. also found that the oligomerization rate is more rapid at near neutral pH.[38] Overall, this pH-dependent behavior is consistent with the silicate particle growth mechanism at larger scales (several or tens of nanometers) reported experimentally.[47,48]

Low pH. We also investigated silicate oligomerization under acidic conditions. The variations in concentration of key silicate species at pH 6 are shown in Figure 9. The processes of formation and consumption of dimers and trimers are faster than those under the other conditions studied above. The system finishes phase A after only 0.02 s. The linear tetramers are formed quickly, while their consumption is much slower. This indicates that lower pH favors the formation of linear tetramers. Perhaps further linear growth is also favorable at low pH. However, in this work the linear tetramer is the largest linear species.

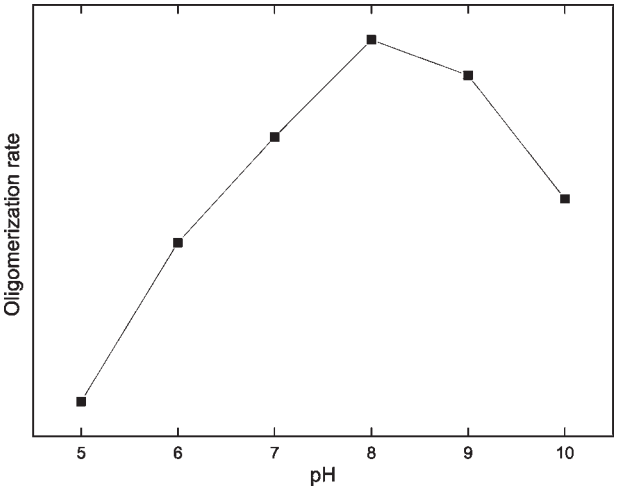

Figure 10. Effects of pH value on the silicate oligomerization rate.

Although a great deal of linear trimers are formed early, they prefer further linear growth. Formation of 3-rings is then unfavorable under these conditions. The transformation from linear tetramer to 4-ring is very slow. The system needs more than 6000 s to finish phase B, which is much slower compared to the cases of higher pH. The rate-determining step is thus 4-ring formation.

We decreased the pH further to 5 (data not shown). Only a few 4-rings are observed after thousands of seconds. The system

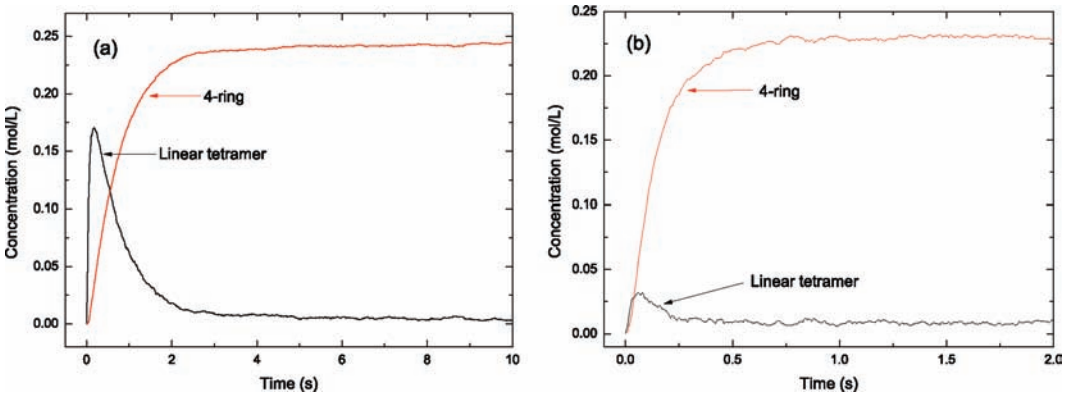

Figure 11. Formation of 4-rings at pH 7 (explicit-water model) and temperatures 400 K (a) and 450 K (b).

is dominated by linear species. The effect of pH on the rate of linear growth can be seen by comparing the maximum values of concentration of linear tetramers. The results in this subsection reveal that low pH favors linear growth, while ring closure becomes unfavorable. As the pH increases, more of the neutral silicate species become ionized. A consequence of this is a significant increase in the possibility of both linear growth through the anionic mechanism and ring closure. As the pH increases further, most of the silicate species are ionized, which however increases the activation barrier of linear growth again.

The pH-dependent silicate oligomerization found in this work is in excellent agreement with previous experimental works.[48] Lin et al. found that the hydrolysis and condensation rate of the silica species are pH dependent. They plotted the effects of pH value on the silicate condensation rate. At pH >2, the condensation rate increases with pH until pH 8 and then decreases again. Under acidic conditions, silica species are the less condensed linear oligomers, while in alkaline solution the silica species are the more cross-linked clusters.[48] In this work, although the length scales are different, we found the same trend. Figure 10 shows the effects of pH value on the silicate oligomerization rate. The silicate oligomerization rate is the fastest at pH 8, and the rate decreases with an increase or decrease of pH. We also found that the linear oligomers are favored under acidic conditions, while ring species are favored under alkaline conditions. These phenomena are due to the fact that the pH controls the distribution of neutral and anionic species and consequently determines the oligomerization rate and species population. At low pH, most of the species are neutral, and thus ring closure is unfavorable. This is the reason that silica species are the less condensed linear oligomers under acidic conditions. The silicate species become ionized under alkaline conditions, which favors ring closure. The total growth is the combination of linear growth and ring closure. Results show that the distribution at pH 8 is optimum for the total growth rate of silicate oligomers.

Temperature Effect. Usually, formation of zeolite crystals occurs upon heating of the solution, making temperature a key variable to be studied. The temperature effects are introduced into this model via the transition state theory (TST). Zhdanov[49] reported the first measurements on crystal linear growth rates and showed directly for the first time the effect of temperature in increasing growth rate. Experimental studies showed that the average particle sizes increase with temperature.[45] Theoretical works also found that increasing the temperature allows for further silica particle growth.[24] In this work, in addition to an

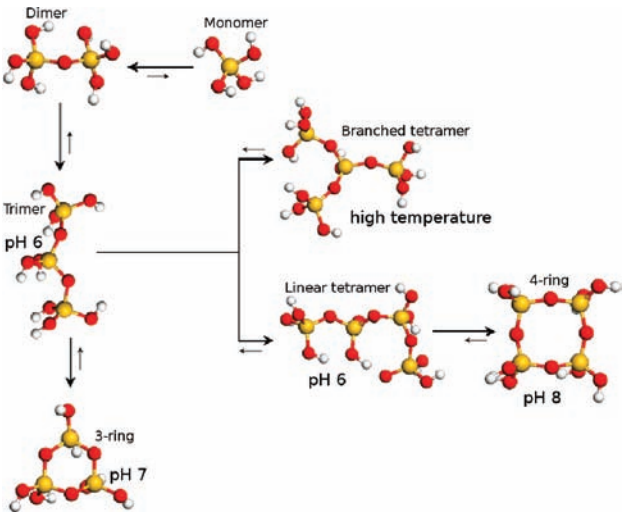

Figure 12. Summary of the preferred conditions for the formation of key species. The pH range considered is 5−10.

increase in the growth rate, the temperature is found to alter the pathway of oligomerization. However, we cannot compare with the previous studies upon the cluster sizes.

In comparison to the case of 350 K, both the linear growth and the ring closure are faster at high temperature. The concentration of 3-rings does not follow that of linear trimer, as shown in the Supporting Information. This means that the temperature 400 K does not favor 3-ring formation. 3-rings are unstable at high temperatures. Meanwhile, 400 K favors formation of 4-rings, as shown in Figure 11. This indicates that the silicate condensation rate is increased by increasing the temperature to 400 K.

450 K is also in the range of typical temperatures of zeolite synthesis.[11] Interestingly, the maximum value of concentration of linear tetramers is greatly reduced at 450 K. The concentration curves for linear tetramers indicate a substantial difference in the growth pathway at different temperatures. At low temperature, the small silicate species first transformed into linear tetramers, and the second step is 4-ring formation. At higher temperature, the linear growth and ring closure occur simultaneously. For the formation of 4-rings, the overall concentration trend is similar to that at lower temperature. The difference is that the ring closure occurs more rapidly at high temperature. Phase B only takes about 1 s. Here we conclusively demonstrate that the overall

dx.doi.org/10.1021/ja110357k |*J. Am. Chem. Soc.* 2011, 133, 6613–6625

silicate oligomerization rate increases with temperature. When the temperature is increased to 450 K, we see a few more branched tetramers formed.

Preferred Conditions. The pH was reported to control the stability of silica nanoparticles and, hence, determines their size distribution on the scale of nanoparticles.[24] Here we report the pH-controlled distributions of small silicate oligomers. In solution, monomeric silicate molecules undergo condensation reactions that lead to the formation of silicate oligomers, which depends on the conditions (mainly pH and temperature) of the solutions. Figure 12 gives a schematic of how each oligomer could be built up from the monomers and summarizes the preferred conditions of key silicate species. The reactant complexes and intermediate species are omitted for clarity. The preferred conditions are the most favorable conditions at which a certain type of silicate oligomer is formed. The silicate oligomerization under various conditions (pH ranges from 5 to 10) have been studied. The preferred condition for the dimer is a low pH value of 6. It is noteworthy that the linear species prefer low pH, while ringed species prefer higher pH. This compares well with previous theoretical works. Wu and Deem reported that the pH value affects the critical cluster size and the nucleation barrier through the oxygen chemical potential.[16] They found that a decrease of pH leads to favorable dimerization. Malani et al. found that a high concentration of OH groups favors ring formation.[20] The oligomerization is a combined action of linear growth and ring closure. Therefore, the pH at which the rate of silicate oligomerization is most rapid is neither very high nor very low. Form the discussions above, the preferred pH lies between 6 and 8 for different species. This is in agreement with experimental results again. Experimentally, the silicate oligomerization rate is most rapid at near pH = 8.[47,48] The formation of branched tetramers can be favored at a temperature of 450 K, as described in the last subsection. The preferred conditions for the key species of the early stage of zeolite formation are obtained, which can accelerate this stage.

CONCLUSIONS

Most importantly, we have developed a continuum (off-lattice) kinetic Monte Carlo model to study the oligomerization reactions of large-scale silicate-solution systems, which opens the way to study many other important problems occurring in solutions on the atomic length and macroscopic time scale. The present study demonstrates that continuum kMC theory is able to provide detailed information regarding the early stage of zeolite formation. Comparing continuum kMC and mean field approximations on the silica-solution system, we conclude that the mean field approximation is rate-limited by intermediate species. Results reveal that the COSMO model is not adequate in modeling silicate oligomerization from water solution, and thus water molecules have to be considered explicitly. We demonstrate that pH and temperature greatly influence the oligomerization rate and pathway. Therefore, silicate oligomerization can be controlled by varying the pH and temperature of the solution. A significant finding is that near neutral pH favors linear growth, because the linear growth is mainly driven by an anionic mechanism in which there is one neutral and one anionic reactant, while a higher pH makes the silicate species anionic, which facilitates ring closure. In the case of pH 7, the species oligomerize first to linear tetramers and then close to form 4-rings, while at high pH the linear growth and ring closure occur simultaneously. The total growth rate is a interplay between linear growth and ring closure. pH 8 is found to be the optimum value that takes care of both linear growth and ring closure, and hence the silicate oligomerization is the fastest at pH 8. The decrease of cluster size with pH is due to the fact that the double-anionic mechanism operable is very slow. The rate-determining steps are ring closure, at very low pH, and linear growth, at very high pH. Preferred conditions necessary for effective oligomerization that can accelerate the initial stage of silicate oligomerization and as a result avoid the formation of undesired species have been obtained.

Future work is planed to take into account the effects of template molecules and larger oligomers.

ASSOCIATED CONTENT

Supporting Information. Text, tables, and figures giving computational details, complete ref 31, linear growth and 3-ring formation at temperatures of 400 and 450 K, and the energies and coordinates of the atoms. This material is available free of charge via the Internet at http://pubs.acs.org.

AUTHOR INFORMATION

Corresponding Author
a.p.j.jansen@tue.nl

ACKNOWLEDGMENT

This work was supported by The Netherlands Organisation for Scientific Research (NWO) as part of the ECHO project No. 700.56.021 "Kinetic Monte Carlo simulations of zeolite synthesis".

REFERENCES

(1) Jorge, M.; Gomes, J. R. B.; Cordeiro, M. N. D. S.; Seaton, N. A. *J. Am. Chem. Soc.* **2007**, *129*, 15414.
(2) Auerbach, S. M.; Ford, M. H.; Monson, P. *Curr. Opin. Colloid Interface Sci.* **2005**, *10*, 220.
(3) Iler, R. K. *The Chemistry of Silica*; Wiley: New York, 1979.
(4) de Moor, P. P. E. A.; Beelen, T. P. M.; van Santen, R. A.; Davis, M. E. *Chem. Mater.* **1999**, *11*, 36.
(5) Mora-Fonz, M. J.; Catlow, C. R. A.; Lewis, D. W. *Angew. Chem., Int. Ed.* **2005**, *44*, 3082.
(6) van Santen, R. A. *Nature* **2006**, *444*, 46.
(7) Erdemir, D.; Lee, A. Y.; Myerson, A. S. *Acc. Chem. Res.* **2009**, *42*, 621.
(8) de Moor, P. P. E. A.; Beelen, T. P. M.; van Santen, R. A. *J. Phys. Chem. B* **1999**, *103*, 1639.
(9) de Moor, P. P. E. A.; Beelen, T. P. M.; van Santen, R. A.; Beck, L. W.; Davis, M. E. *J. Phys. Chem. B* **2000**, *104*, 7600.
(10) Knight, C. T. G. *J. Chem. Soc., Dalton Trans.* **1988**, 1457.
(11) Catlow, C. R. A.; Bromley, S. T.; Hamad, S.; Mora-Fonz, M.; Sokol, A. A.; Woodley, S. M. *Phys. Chem. Chem. Phys.* **2010**, *12*, 786.
(12) Pelster, S. A.; Schrader, W.; Schth, F. *J. Am. Chem. Soc.* **2006**, *128*, 4310.
(13) Depla, A.; Lesthaeghe, D.; van Erp, T. S.; Aerts, A.; Houthoofd, K.; Fan, F.; Li, C.; Speybroeck, V. V.; Waroquier, M.; Kirschhock, C. E. A.; Martens, J. A. *J. Phys. Chem. C* **2011**, *115*, 3562.
(14) Fan, F.; Feng, Z.; Li, C. *Acc. Chem. Res.* **2010**, *43*, 378.
(15) Pereira, J. C. G.; Catlow, C. R. A.; Price, G. D. *Chem. Commun.* **1998**, 1387.
(16) Wu, M. G.; Deem, M. W. *J. Chem. Phys.* **2002**, *116*, 2125.
(17) Schumacher, C.; Seaton, N. A. *Adsorption* **2005**, *11*, 643.

(18) Schumacher, C.; Gonzalez, J.; Wright, P. A.; Seaton, N. A. *J. Phys. Chem. B* **2006**, *110*, 319.
(19) Schumacher, C.; Gonzalez, J.; Perez-Mendoza, M.; Wright, P. A.; Seaton, N. A. *Ind. Eng. Chem. Res.* **2006**, *45*, 5586.
(20) Malani, A.; Auerbach, S. M.; Monson, P. A. *J. Phys. Chem. Lett.* **2010**, *1*, 3219.
(21) Auer, S.; Frenkel, D. *Nature* **2001**, *409*, 1020.
(22) ten Wolde, P. R.; Ruiz-Montero, M. J.; Frenkel, D. *Phys. Rev. Lett.* **1995**, *75*, 2714.
(23) Doye, J. P. K.; Frenkel, D. *J. Chem. Phys.* **1999**, *110*, 2692.
(24) Jorge, M.; Auerbach, S. M.; Monson, P. A. *J. Am. Chem. Soc.* **2005**, *127*, 14388.
(25) Trinh, T. T.; Jansen, A. P. J.; van Santen, R. A. *J. Phys. Chem. B* **2006**, *110*, 23099.
(26) Trinh, T. T.; Jansen, A. P. J.; van Santen, R. A.; Meijer, E. J. *Phys. Chem. Chem. Phys.* **2009**, *11*, 5092.
(27) Rao, N. Z.; Gelb, L. D. *J. Phys. Chem. B* **2004**, *108*, 12418.
(28) Zhang, X.-Q.; Jansen, A. P. J. *Phys. Rev. E* **2010**, *82*, 046704.
(29) Erp, T. S. V.; Caremans, T. P.; Kirschhock, C. E. A.; Martens, J. A. *Phys. Chem. Chem. Phys.* **2007**, *9*, 1044.
(30) Lukkien, J. J.; Segers, J. P. L.; Hilbers, P. A. J.; Gelten, R. J.; Jansen, A. P. J. *Phys. Rev. E* **1998**, *58*, 2598.
(31) Frisch, M. J. *Gaussian 03*; Gaussian, Inc., Wallingford, CT, 2004.
(32) Car, R.; Parrinello, M. *Phys. Rev. Lett.* **1985**, *55*, 2471.
(33) Schaffer, C. L.; Thomson, K. T. *J. Phys. Chem. C* **2008**, *112*, 12653.
(34) Jorge, M.; Auerbach, S. M.; Monson, P. A. *Mol. Phys.* **2006**, *104*, 3513.
(35) Tossell, J. A. *Geochim. Cosmochim. Acta* **2005**, *69*, 283.
(36) Robson, H. *International Zeolite Association*, 2nd ed.; Elsevier: Amsterdam, 2001.
(37) Knight, C. T. G.; Kinrade, S. D. *J. Phys. Chem. B* **2002**, *106*, 3329.
(38) Icopini, G. A.; Brantley, S. L.; Heaney, P. J. *Geochim. Cosmochim. Acta* **2005**, *69*, 293.
(39) Pereira, J. C. G.; Catlow, C. R. A.; Price, G. D. *J. Phys. Chem. A* **1999**, *103*, 3268.
(40) Jorge, M.; Gomes, J. R. B.; Cordeiro, M. N. D. S.; Seaton, N. A. *J. Phys. Chem. B* **2009**, *113*, 708.
(41) Trinh, T. T.; Jansen, A. P. J.; van Santen, R. A.; VandeVondele, J.; Meijer, E. J. *ChemPhysChem* **2009**, *10*, 1775.
(42) Cho, H.; Felmy, A. R.; Craciun, R.; Keenum, J. P.; Shah, N.; Dixon, D. A. *J. Am. Chem. Soc.* **2006**, *128*, 2324.
(43) Gomes, J. R. B.; Cordeiro, M. N. D. S.; Jorge, M. *Geochim. Cosmochim. Acta* **2008**, *72*, 4421.
(44) Knight, C. T. *Zeolites* **1990**, *10*, 140.
(45) Fedeyko, J. M.; Rimer, J. D.; Lobo, R. F.; Vlachos, D. G. *J. Phys. Chem. B* **2004**, *108*, 12271.
(46) Yang, S.; Navrotsky, A.; Wesolowski, D. J.; Pople, J. A. *Chem. Mater.* **2004**, *16*, 210.
(47) Tleugabulova, D.; Duft, A. M.; Zhang, Z.; Chen, Y.; Brook, M. A.; Brennan, J. D. *Langmuir* **2004**, *20*, 5924.
(48) Lin, H.-P.; Mou, C.-Y. *Acc. Chem. Res.* **2002**, *35*, 927.
(49) Zhdanov, S. P. *ACS Adv. Chem. Ser.* **1971**, *101*, 20.